7-2006

Temporal dynamics of the urban heat island of Singapore

Winston T. L. CHOW
Singapore Management University, winstonchow@smu.edu.sg

Matthias ROTH
National University of Singapore

Citation

CHOW, Winston T. L., & ROTH, Matthias.(2006). Temporal dynamics of the urban heat island of Singapore. *International Journal of Climatology, 26(15)*, 2243-2260.
Available at: https://ink.library.smu.edu.sg/soss_research/3068

INTERNATIONAL JOURNAL OF CLIMATOLOGY
Int. J. Climatol. **26**: 2243–2260 (2006)
Published online 12 July 2006 in Wiley InterScience
(www.interscience.wiley.com) DOI: 10.1002/joc.1364

RMetS
ROYAL METEOROLOGICAL SOCIETY

TEMPORAL DYNAMICS OF THE URBAN HEAT ISLAND OF SINGAPORE

WINSTON T. L. CHOW* and MATTHIAS ROTH
Department of Geography, Faculty of Arts and Social Sciences, National University of Singapore, Singapore

Received 23 November 2005
Revised 25 April 2006
Accepted 28 April 2006

ABSTRACT

The temporal variability of the canopy-level urban heat island (UHI) of Singapore is examined for different temporal scales on the basis of observations during a 1-year period. Temperature data obtained from different urban areas (commercial, Central Business District (CBD), high-rise and low-rise housing) are compared with 'rural' reference data and analysed with respect to meteorological variables and differences in land use. The results indicate that the peak UHI magnitude occurs 3–4 h (>6 h) after sunset in the commercial area, (at other urban sites). Higher UHI intensities generally occur during the southwest monsoon period of May–August, with a maximum of ~7 °C observed in the commercial area under ideal meteorological conditions. Variations in seasonal precipitation explain some of the differences in urban–rural cooling. No clear relationship between urban geometry and UHI intensity can be seen, and intra-urban variations of temperature are also shown to be influenced by other site factors, e.g. the extent of green space and anthropogenic heat. Lastly, results from the present study are compared with UHI data from other tropical and mid-latitude cities. Copyright © 2006 Royal Meteorological Society.

KEY WORDS: urban heat island; tropical urban climate; temperature; Singapore

1. INTRODUCTION

Perhaps the clearest illustration of human impact on synoptic-scale climate is the urban heat island (UHI) phenomenon, i.e. the increase of the sub-surface, surface, or air temperatures observed in an urban environment compared to the undeveloped rural surroundings (e.g. Landsberg, 1981). Several factors have been postulated to explain the extra warmth of cities. They are (1) increased absorption of short-wave radiation, (2) increased storage of sensible heat, (3) anthropogenic heat production, (4) reduced long-wave radiation losses, (5) lower evapotranspiration rates, and (6) lower sensible heat loss due to reduced turbulence in urban canyons (Oke, 1987). Other factors, such as synoptic weather conditions (e.g. wind speed, cloud amount and height) (Oke, 1998), topography (Goldreich, 1984), city morphology, and size (Oke, 1973) modify the magnitude of UHI intensity, which is defined as the temperature difference between the urban area (T_u) and its rural (T_r) surroundings ($\Delta T_{u-r} = T_u - T_r$). Observations from cities located in temperate climates show that UHI intensity varies in a consistent manner during a 24-h period (Oke, 1982; Runnalls and Oke, 2000). Generally, air temperature decreases from late afternoon and evening, with urban areas cooling at lower rates than rural areas. This difference results in the growth of ΔT_{u-r} until a maximum is reached at about 3–5 h after sunset. The UHI gradually declines later at night and disappears after sunrise owing to the rapid warming of rural areas. These general UHI characteristics are best displayed during calm and clear weather conditions when the highest UHI magnitudes (UHI_{MAX}) are measured.

Numerous studies have been undertaken to document the UHI of cities in temperate regions (e.g. Chandler, 1965; Oke and Maxwell, 1975; Ackerman, 1985; Magee *et al.*, 1999; Runnalls and Oke, 2000).

* Correspondence to: Winston T. L. Chow, School of Geographical Sciences, Arizona State University, P.O. Box 870104, Tempe, AZ 85287-0104 United States of America; e-mail: winston.chow@asu.edu

Similar information is scarcer for tropical cities, but there are a few notable studies (e.g. Jauregui, 1973; Padmanabhamurty, 1979; Sham, 1987; Jauregui, 1997; Deosthali, 2000). From these results, two major differences between the UHI of temperate and tropical cities can been noted. First, tropical UHI_{MAX} intensities are generally lower than those observed in temperate cities of similar population size (Jauregui, 1986a; Oke *et al*., 1991). Second, UHI_{MAX} in tropical cities occurs later than that observed in temperate cities at around midnight (Jauregui, 1986b; Jauregui *et al*., 1992), or near dawn (Padmanabhamurty, 1979; Jauregui, 1997; Deosthali, 2000).

Despite the general lack of tropical UHI studies, Singapore has a relatively long history of UHI research. The first known results were presented by Nieuwolt (1966), who noted a UHI_{MAX} of ~4.5 °C at 23:00 local time (LT) on a clear and calm night. On cloudy and windy conditions, UHI intensities were lower (~1.5 °C). However, this study was restricted to point measurements taken in the south of the island during a few nights in October. The spatial extent of the UHI of the entire island was investigated by the Singapore Meteorological Service (SMS, 1986) from several observations of $\mathbf{\Delta} T_{u-r}$ conducted at 22 : 00 LT during different times of the year using a combination of fixed sites and vehicle traverses. A large persistent warm belt covering the Central Business District (CBD), residential, and industrial areas was observed. Pockets of cool regions were measured in less-developed outskirts, as well as in the forested central water catchment. UHI_{MAX} was ~5 °C during drier mid-year months. Lower UHI intensities (<2.5 °C) were observed during December and January. Goh and Chang (1998) also conducted a UHI study of similar scale and duration. The warm belt was still present, with UHI_{MAX} of 4.8 °C again found in July compared to UHI magnitudes of ~3.5 °C in March and September, and 2.5 °C in January. However, they discovered that the spatial extent of the UHI had increased as more undeveloped areas became urbanised, i.e. areas that were previously marshlands or mangroves were converted to residential areas. A recent survey of the nocturnal UHI was conducted by Wong and Yu (2005). They found a UHI of ~4 °C, measured as the difference between the CBD and the forested central catchment based on one island-wide traverse carried out in September between 02 : 00–04 : 00 LT. The impact of vegetation on the UHI was illustrated, with lower temperatures observed in built-up areas with more green space.

While these studies have yielded important results, several questions still remain unanswered. Because most studies were conducted at ~22 : 00 LT, the timing of UHI_{MAX} is unknown. The UHI is a dynamic feature, and analyses of differing urban and rural cooling rates is key to understanding UHI causation (e.g. Ludwig, 1970; Oke and Maxwell, 1975). The objectives of this paper therefore are to observe and document diurnal and seasonal variations of the canopy-level UHI intensity in Singapore over a 1-year period. The results are related to variations in land-use and meteorological factors, as well as to surface moisture conditions. Finally, the paper will conclude by comparing the present results with previous work from temperate and tropical studies.

2. STUDY AREA AND METHODOLOGY

2.1. Study area

Singapore is an island state located between 1°09′N to 1°29′N, and 103°36′E to 104°25′E. Population of this densely built-up country was about 4 million in 2003. It has a typical wet equatorial climate with uniformly high annual mean temperatures (26–27.5 °C) and rainfall (~2300 mm) (Köppen classification = *Af*) (Figure 1). The higher monthly precipitation values observed between November and January are associated with the NE monsoon. Relatively drier periods occur during the SW monsoon (May–July). The impact of the monsoons alters cloudiness, surface wind speed, and wind direction, producing distinct seasonal patterns, with higher surface wind speeds from November to February and consistent surface winds from NE between December and March. On the other hand, surface winds are generally from south to southeast between May and September. Given these characteristics, the climate is sometimes divided into four seasons: northeast and southwest monsoons, separated by two brief inter-monsoon or pre-monsoon periods (Chia and Foong, 1991). The absence of large and pronounced topography (the highest point, located in the centre of

DOI: 10.1002/joc

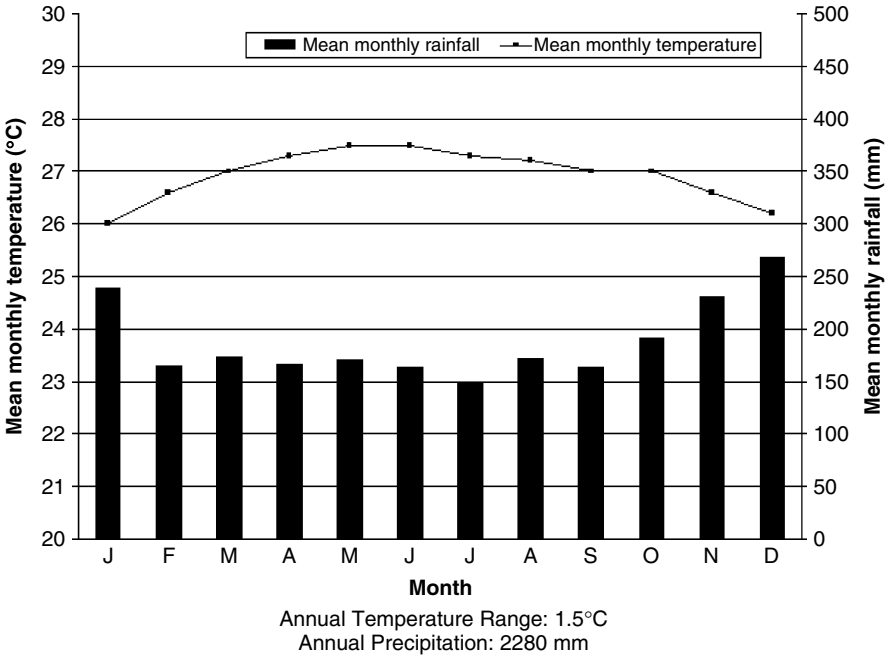

Figure 1. Climograph of Singapore based on data from 1872 to 1988 measured at Paya Lebar Airbase (Source: Singapore Meteorological Service, 1967–1988)

the island, is only 164 m a.s.l.) and the small size of the main island ($\sim$605 km^2) result in a lack of major variation in local the synoptic climate.

In contrast to the lack of spatial variation in climate, Singapore has undergone rapid changes in physical landscape over the last 40 years primarily due to the implementation of concerted governmental urban development policies. The amount of built-up area has almost doubled from 28% to 50%, with a corresponding large decrease in farm area and minor loss of forest spaces (Figure 2). Much of this urbanisation was associated with construction of high-rise public housing estates across much of the island. Rapid development of office/commercial high-rise buildings also took place in the CBD located in the south. Drainage of swamps in the west was carried out to construct industrial factories, and land reclamation progressively expanded the southern coastline. The only remaining significant rural areas are pockets of tropical rainforest in the central catchment and undeveloped areas in the northwest, primarily used for military training and farming (Figure 3).

2.2. Observation sites and instrumentation

Observation sites were selected to represent a wide range of urban morphologies, which included the predominant types of residential areas in Singapore. Two sites were chosen in the city centre (Figure 3). One was in the commercial area (COM) where past measurements have observed the UHI_{MAX} (e.g. SMS, 1986; Goh and Chang, 1998). This station was located at the centre of the commercial and shopping area of Orchard Road. Another station (CBD) was sited in the financial/CBD located near the southernmost tip of the island, which is dominated by closely spaced skyscrapers of $z > 150$ m (where $z =$ height above ground). Another station (HDB) was located in a government-built housing development board (HDB) estate, characterised by high-rise flats of $z = 35$–40 m. Similar HDB estates are spread throughout the island and house about 85% of the population. A low-rise housing area consisting of 2–3 storey, privately owned, terrace houses was selected as the second residential site (RES). Both residential sites were approximately the same distance from the coast (1.5 km). The main morphological characteristics of all sites are summarised in Table I, with corresponding photographs in Figure 4. The general land use did not vary greatly within a 500 m circle

DOI: 10.1002/joc

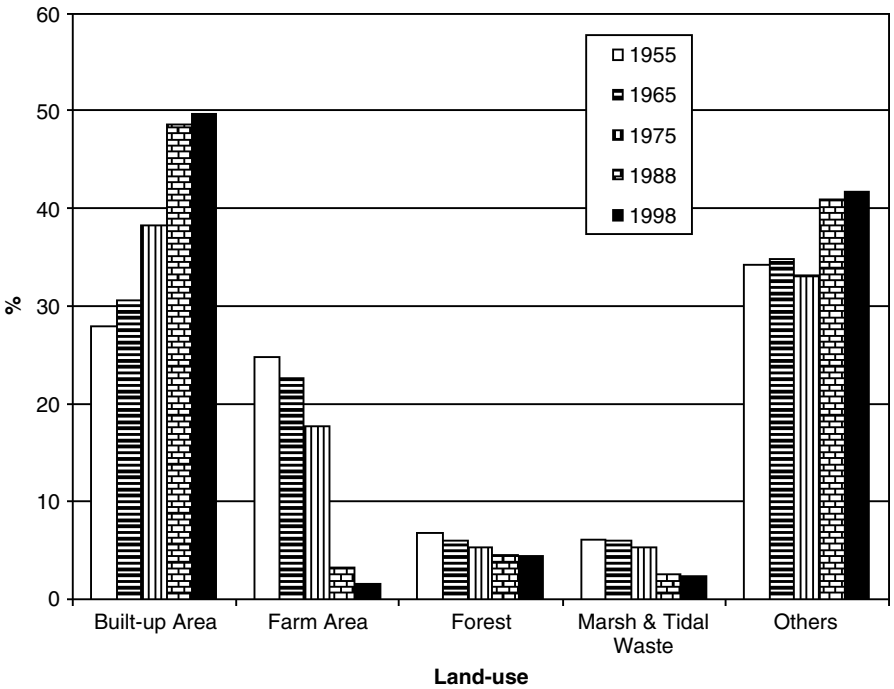

Figure 2. Land-use in Singapore between 1955 and 1998. 'Others' includes inland water (e.g. reservoirs), open spaces, public gardens, cemeteries, military establishments, and unused land (Source: Department of Statistics, 1998)

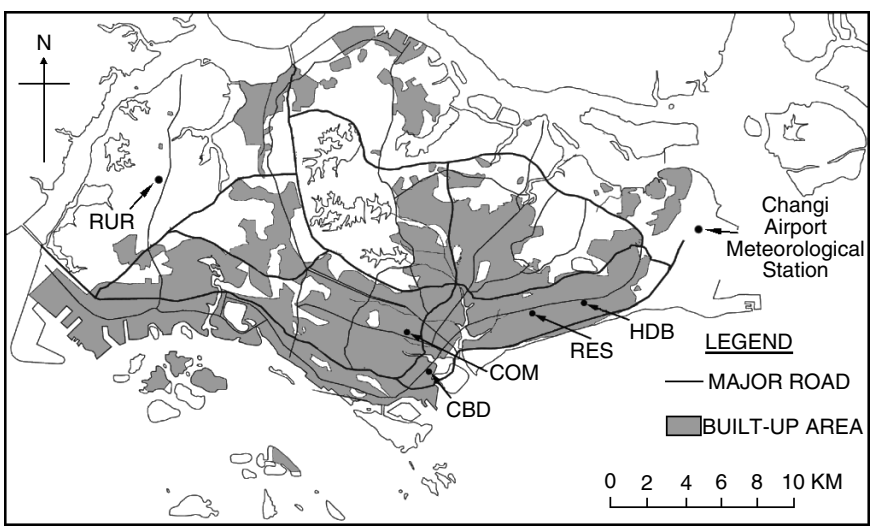

Figure 3. The extent of built-up area in 2002, indicated by the gray shaded area. Also shown are the locations of the observation sites (black dots) and MSD Changi Airport meteorological station. COM, commercial area; CBD, Central Business District; HDB, high-rise residential flats; RES, low-rise residential estate; RUR, undeveloped 'rural' area in secondary tropical rainforest

centred on the actual site. This homogeneity helps us to ensure that the observations are representative of the microclimate of the particular land use (Runnalls and Oke, 2000).

Selection of an appropriate rural site was more difficult. Ideally, following the Lowry (1977) framework, the rural site should reflect pre-urban conditions unaffected from topographic or coastal influences. This

DOI: 10.1002/joc

Table I. Summary of site characteristics

Site/instrument height	General urban characteristics of site (within 500 m radius)	General vegetation characteristics of site (within 500 m radius)	Vegetation index (%)	Distance from nearest coastline (km)	H/W ratio within 500 m radius	SVF
COM/4.5 m	Commercial buildings ($z = 30$–40 m), shopping malls, office blocks, hotels, multi-story car parks; mixture of two- and five-lane roads	Isolated trees ($z = 5$ m); several small (10–20 m^2) grass patches	23	3.7	2–7	0.153
CBD/4.5 m	Tall office buildings ($z = 280$ m), multi-story car parks; wide four-lane roads	1 m shrubs and 5 m trees planted at regular intervals; 0.5 ha open grass park located 200 m E from site	17	0.5 (0.2 km from river)	10–18	0.108
HDB/4 m	High-rise residential flats ($z = 35$–40 m), open car parks with tarmac surface; mixture of two- and four-lane roads	1 ha park 100 m W from site; numerous small grass patches (10–20 m^2), 5 m trees planted at regular intervals throughout estate	64	1.5	2.5–3	0.322
RES/3 m	Low-rise private terrace housing ($z = 10$ m); narrow two-lane roads	2–3 m trees planted at regular intervals along road; small garden space (20–30 m^2) in front of houses	38	1.5	0.5–1	0.511
RUR/2 m	Chicken farms ($z = 10$ m); gravel tracks	Secondary tropical dipterocarp rainforest; 10–20 m mature trees; dense undergrowth in clearings (20–50 m^2)	95	3 (2.5 km from lake)	N.A.	0.440

Vegetation index is calculated as the amount of green space (i.e. trees, shrubs, grass, soils) within a 500 m radius of each site; SVF, sky view factor, measured at the height of sensor; z, the height above ground; N.A., not applicable.

DOI: 10.1002/joc

Figure 4. Photographs of land-use characteristics at each site. Clockwise from top left: commercial (COM); Central Business District (CBD); high-rise residential flats (HDB); undeveloped secondary tropical rainforest (RUR); low-rise residential private estate (RES)

would be the primary tropical rainforest in the present case. However, the remaining primary rainforest is confined to a nature reserve in a small, hilly area in the centre of the island and hence is unsuitable. Instead, a large relatively less developed area consisting of a mix of secondary tropical rainforest, agricultural land, and military training grounds in the NW of the island was chosen as the rural (RUR) site. The area close to the actual site consists of dipterocarp trees of $z = 10–20$ m, frequently interspersed with dense undergrowth in small clearings. The instruments were sited in one such clearing ($\sim$40 m^2) which was assumed to be a suitable rural or undeveloped reference location. The only urban structures within 500 m of the site were three chicken farms ($\sim 50 \times 10$ m; $z = 10$ m) located 300–350 m E. The elevation of the station was about 30 m a.s.l., with the nearest significant water body approximately 2.5 km W (Figure 3).

Temperature (T), wind speed (u), and direction (θ) at COM, CBD, HDB, and RES were measured using a Vaisala HMP45A sensor and a Campbell Scientific (CSI) Met-One 034B sensor. T at RUR was also measured with a HMP45A sensor, but u and θ were obtained with Met-One 014 and 024 sensors, respectively. Additional observations at RUR included rainfall using a CSI TB4 rainfall gauge, and net radiation with a Q-7.1 net radiometer. Signals were sampled every 10 s, and 20 min averages written to CSI CR510 (all urban sites) and CR10X (RUR) data loggers. Calibration of instruments was done before and after fieldwork to ensure data accuracy. Comparisons showed small systematic errors in T ($<0.15\,^{\circ}$C) between individual sensors, which were subsequently adjusted for.

In all urban sites, sensors were mounted at the end of a 2 m boom attached to lamp-posts with booms positioned towards the street canyon centre. No guidelines are available regarding either the optimal height above surface level or the exposure of sensors in urban environments, although this topic has recently been addressed by Oke (2004). To avoid vandalism, theft, or traffic interference, sensors were placed 3–4.5 m above surface level (Table I). This is higher than the World Meteorological Organisation's (WMO) guideline of 2 m for rural stations (WMO, 1971). However, past observations in urban canyons have shown that mixing of air is sufficient to maintain neutral stratification (Taesler, 1980), and T differences are usually $<0.5\,^{\circ}$C and always $<1\,^{\circ}$C under most weather conditions for a canyon of height-to-width ratio (H/W) $\sim$1 (Nakamura and Oke, 1988). Further, in the case of densely built-up urban areas, temperature gradient errors should be minimal if sensors are located at least 1 m from the walls of the urban canyon (Oke, 2004). A brief check also

DOI: 10.1002/joc

showed no vertical T gradients at night between $z = 2$ m and $z = 3$ m at RES. Observations were performed between March 2003 and March 2004 at COM, CBD, and RUR, and between June 2003 and March 2004 at HDB and RES.

Additional data used in the present study include hourly rainfall from rain gauges in close proximity (0.8–2.5 km) to the urban stations maintained by the Meteorological Services Division (MSD), as well as mean surface wind speed ($\overline{u}$) and wind direction ($\overline{\theta}$) at $z = 15$ m and low cloud cover and height ($z \leq 900$ m) measured at the MSD station at Changi Airport (Figure 3). These observations were used assuming that they best represented the synoptic meteorological conditions for Singapore. While it is not ideal to extrapolate these variables for the whole island, there was little alternative, as other MSD stations did not provide contiguous 24-h data for several of these variables. Nonetheless, a comparison of hourly and monthly $\overline{u}$ data from both Changi and the rural stations showed generally similar trends but not necessarily similar magnitudes during the study period.

To enable data comparisons of climate variables between seasons for the observation period, the MSD data, particularly $\overline{u}$, $\overline{\theta}$, and cloud cover from Changi, were analysed to determine the start and end months of each season (Figure 5). Starting from May 2003, $\overline{\theta}$ was predominantly S–SW, switching to N–NE in November 2003 until March 2004. May and November 2003 therefore marked the start of the SW and NE monsoon seasons, respectively. The inter-monsoon periods are known to occur during both equinoxes, and are characterised by frequent afternoon rainstorms, with relatively lower $\overline{u}$ and $\overline{\theta}$ compared to the monsoon seasons (Chia and Foong, 1991). Thus, March–April and September–October were classified as inter-monsoon periods (pre-SW and pre-NE, respectively) and November–February and May–August as monsoon seasons (NE and SW monsoon, respectively) (Table II).

The timing and frequency of rainfall events vary seasonally (Table III). The NE monsoon season generally has high monthly precipitation, with the exception of February, which was the driest month observed. Rainfall events during the SW monsoon season were less frequent. Both inter-monsoon periods had more frequent monthly precipitation events compared to the SW monsoon season, with a high proportion of pre-dawn precipitation recorded in the pre-NE monsoon period. These observations generally mirror the rainfall variation in Figure 1. Table III also shows a high proportion of storms occurring from noon until sunset throughout the year, which is a typical characteristic of convectional rainfall in equatorial climates.

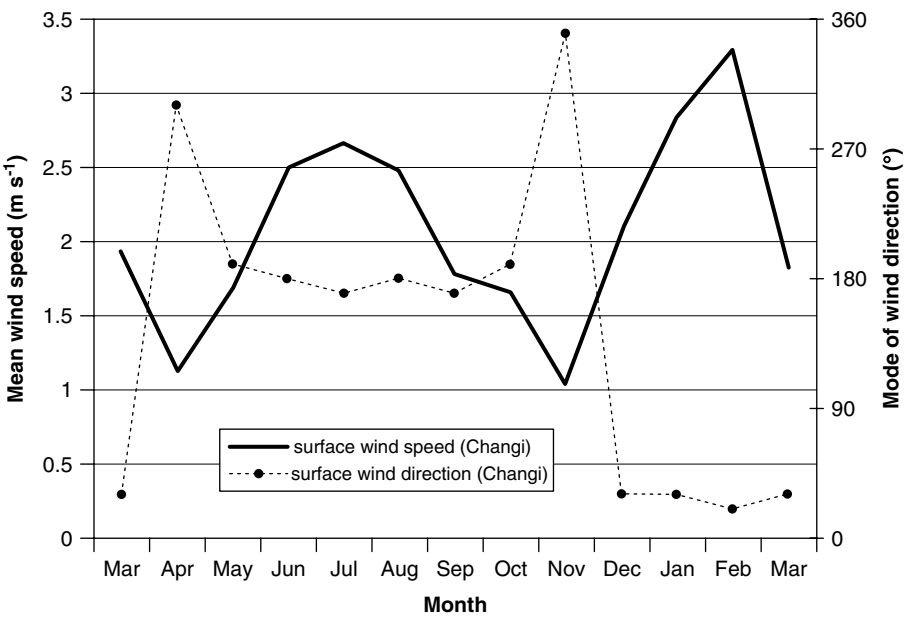

Figure 5. Mean surface wind speed and mode of surface wind direction recorded at MSD Changi station between March 2003 and March 2004

DOI: 10.1002/joc

Table II. Classification of seasons for the observation period (March 2003–March 2004)

Season	Months included	Meteorological conditions
Pre-southwest monsoon (Pre-SW)	March–April 2003; March 2004	Winds from NW to NE; low mean wind speed; frequent afternoon rain, and low mean low-cloud ($z \leq 900$ m) cover
Southwest monsoon (SW)	May–August 2003	Winds from S to SE; lowest seasonal rainfall; slightly greater mean low-cloud and mean wind speeds compared to inter-monsoon periods
Pre-northeast monsoon (Pre-NE)	September–October 2003	Winds from S to SW; low mean wind speed; frequent afternoon rain, with frequent pre-dawn rainfall in October (Sumatran squalls); low mean low-cloud cover
Northeast monsoon (NE)	November 2003–February 2004	Winds predominantly from NE; highest seasonal rainfall (except February); greatest seasonal mean low-cloud cover; highest seasonal mean wind speeds

Table III. Seasonal variation of time (in LT) and frequency of rainfall events during the observation period. Observations were taken from MSD stations closest to each urban station and from RUR. Precipitation events that straddle two time periods are double-counted (e.g. a storm lasting from 00 : 00–12 : 00 is counted in both categories)

Season/month	00 : 00–06 : 00	06 : 00–12 : 00	12 : 00–18 : 00	18 : 00–00 : 00	Total
March 2003	3	3	13	4	23
April 2003	7	5	24	13	49
March 2004	9	8	25	13	55
Pre-SW total	19	16	62	30	127
May 2003	3	8	10	3	24
June 2003	2	7	12	2	23
July 2003	5	10	16	9	40
August 2003	7	13	11	8	39
SW total	17	38	49	22	126
September 2003	6	8	15	4	33
October 2003	11	12	17	5	45
Pre-NE total	17	20	32	9	78
November 2003	8	10	23	5	46
December 2003	3	11	23	10	47
January 2004	9	8	16	11	44
February 2004	0	1	10	3	14
NE total	20	30	72	29	151
Total	73	104	215	90	482

To determine the timing and duration of daytime and nocturnal periods, ephemeris calculations of daily sunrise, mid-day and sunset times were performed for each day. Sunrise occurs from 06 : 50–07 : 10 LT, solar noon between 13 : 00–13 : 10 LT, and sunset between 18 : 50–19 : 10 LT. Given these narrow diurnal ranges typical of an equatorial location, sunrise and sunset times were standardised to 07 : 00 and 19 : 00 LT, respectively. Local apparent time (LAT) was then calculated for solar time accuracy in this study according to the method specified by Oke (1987). On average, LAT is 1 h behind LT, with minor monthly variation ranging from −9.6 to +20.4 min. Given the significant difference between LT and LAT, and to allow for accurate comparisons with other UHI temporal studies, LAT is the time scale used in this paper unless specified otherwise.

DOI: 10.1002/joc

3. RESULTS

The results of the present study are examined over two temporal scales. First, diurnal variations in UHI dynamics are presented to illustrate UHI development during a 24-h period. Second, UHI data is classified according to seasons to illustrate changes of UHI development and magnitudes during different monsoonal and inter-monsoonal periods.

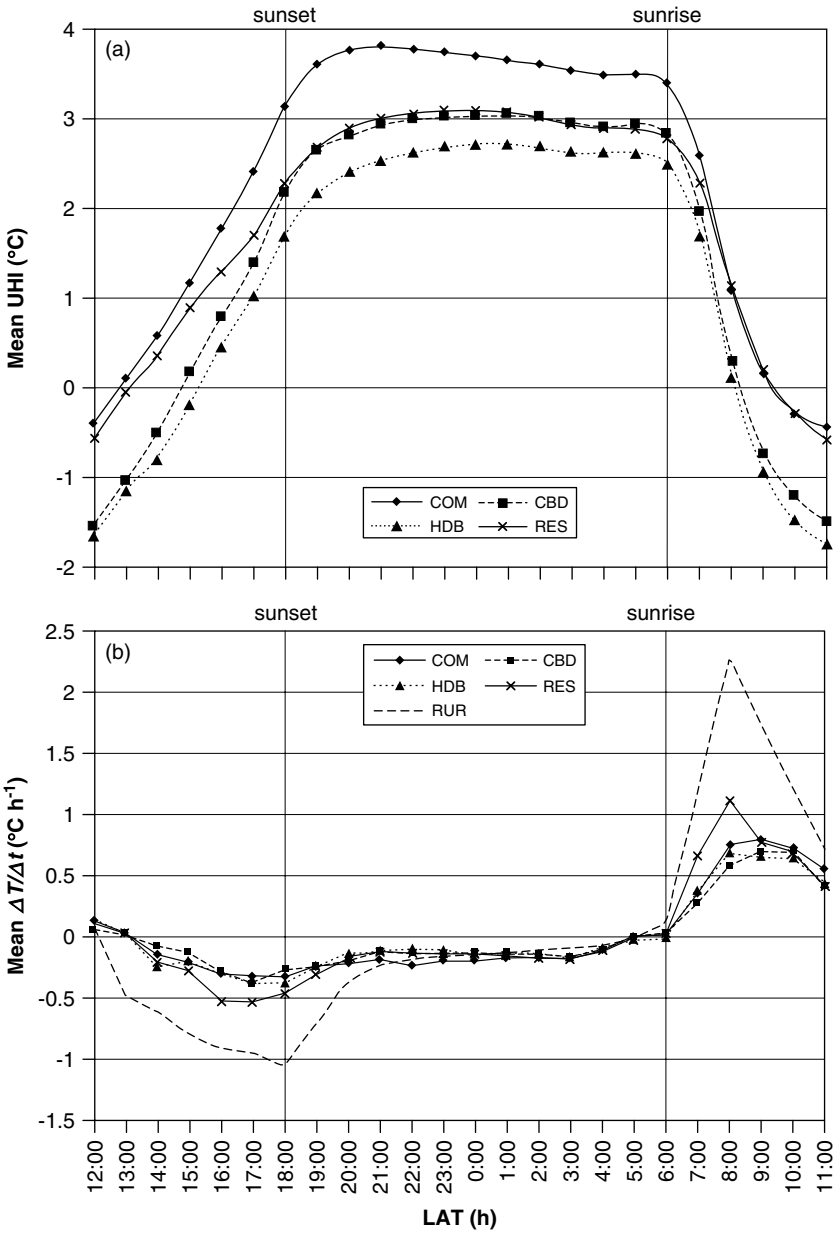

Figure 6. Diurnal variation for all days and meteorological conditions between March 2003 and March 2004 of mean hourly (a) UHI intensity at urban stations and (b) warming/cooling rates ($\Delta T/\Delta t$) at urban and rural stations. COM, commercial site; CBD, Central Business District site; HDB, high-rise residential site; RES, low-rise residential site; RUR, undeveloped 'rural' site in secondary tropical rainforest

DOI: 10.1002/joc

3.1. Diurnal variation of the urban heat island

Ensemble averages of the diurnal variation of UHI intensity for all days and meteorological conditions are plotted in Figure 6(a). Mean UHI intensities were always highest at COM with a maximum value of 3.8 °C at about 21 : 00 h, i.e. 3 h after sunset. The mean UHI at HDB follows a similar diurnal variation, but the magnitudes during night-time are consistently lower compared to other sites, with the peak intensity (2.8 °C) observed later at midnight. The nocturnal UHI for CBD and RES are generally similar both in intensity and in timing of the peak at midnight. The UHI is seen to dissipate rapidly at all sites within 1–2 h after sunrise. All sites exhibit 'cool islands', i.e. negative UHI intensity, during daytime with higher magnitudes around noon. Finally, negative UHI values are most prominent at CBD and HDB, which result in a delayed onset of the UHI at these two sites.

Mean hourly temperature warming/cooling rates ($\Delta T/\Delta t$) were calculated to analyse the temporal development of the UHI (Figure 6(b)). Cooling at all urban sites starts around 14 : 00 h, 1 h later than that observed at the rural station. The growth of the UHI occurs as RUR cools at higher rates than those observed at urban sites from noon to 22 : 00 h, and diurnal UHI attains a maximum intensity when rural and urban cooling rates become equal in magnitude around midnight. After sunrise, RUR experiences much higher warming compared to the urban stations, which results in a rapid decrease of UHI intensity throughout the morning hours.

Magnitudes of rural and urban $\Delta T/\Delta t$ observed in Singapore are much smaller than those found in several temperate cities. For example, peak summer cooling rates of rural (urban) areas under ideal weather conditions were 2.8 °C h^{-1} (1 °C h^{-1}) in Montreal, Canada, and 3 °C h^{-1} (1.5 °C h^{-1}) in Vancouver, Canada (Oke and Maxwell, 1975). Urban cooling rates in these cities also fluctuated throughout the nocturnal period in contrast to the relatively steady rates of cooling observed in Singapore after 21 : 00 h. The present peak urban cooling rates are also smaller than the maximum cooling rate of ~1.8 °C h^{-1} observed in Mexico City, Mexico (Jauregui, 1986b). In addition, the timing of maximum cooling rates in these two tropical cities is different. The peak occurs 1 h after sunset in Mexico City as opposed to 1 h before sunset in Singapore.

3.2. Seasonal variation of the urban heat island

Seasonal variation of mean monthly UHI_{MAX} (i.e. average of all UHI_{MAX} values for all days within a month) for all weather conditions is plotted in Figure 7, with all stations displaying similar seasonal trends.

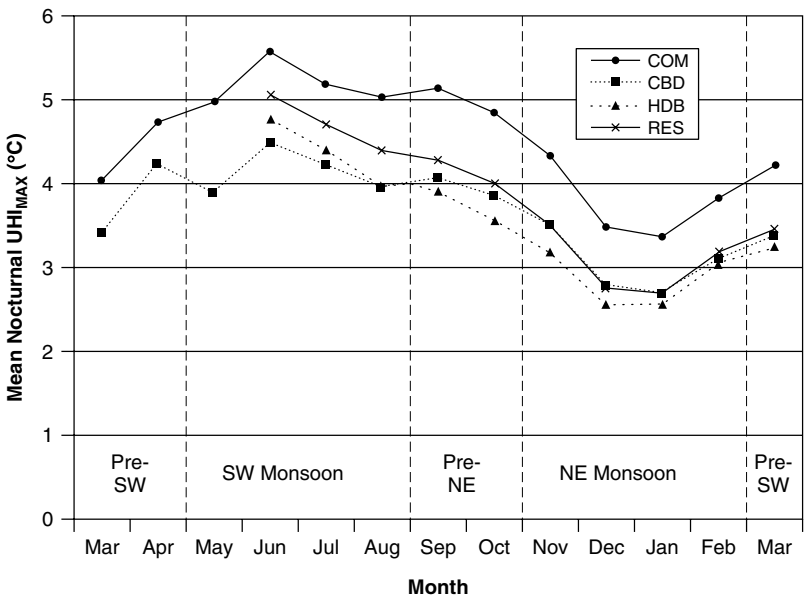

Figure 7. Monthly mean UHI_{MAX} under all weather conditions from four urban stations. No HDB and RES data was available between March and May 2003. Seasons are defined according to Table II

DOI: 10.1002/joc

Magnitudes gradually increased from the pre-SW monsoon season in March 2003 to a peak during the SW monsoon in June, followed by a gradual decline with minimum values measured during the NE monsoon (December–January) before UHI_{MAX} increases again. The order of UHI_{MAX} magnitudes between stations is similar to that observed in Figure 6(a), with the exception of CBD, which shows lower values during the SW monsoon from June to August.

The highest value of UHI_{MAX} was 7.07 °C observed at 21 : 00 h on 17 May 2003, at COM under conditions of light wind (~0.9 m s^{-1}) and no cloud cover. Magnitudes of UHI_{MAX} at other stations were always between 0.3–2 °C lower compared to COM. As largest UHI intensities are consistently measured at COM, data from this station will be analysed in greater detail. This is done by examining nocturnal UHI during ideal synoptic weather conditions of clear and calm weather. Data from COM was screened for nights when mean cloud

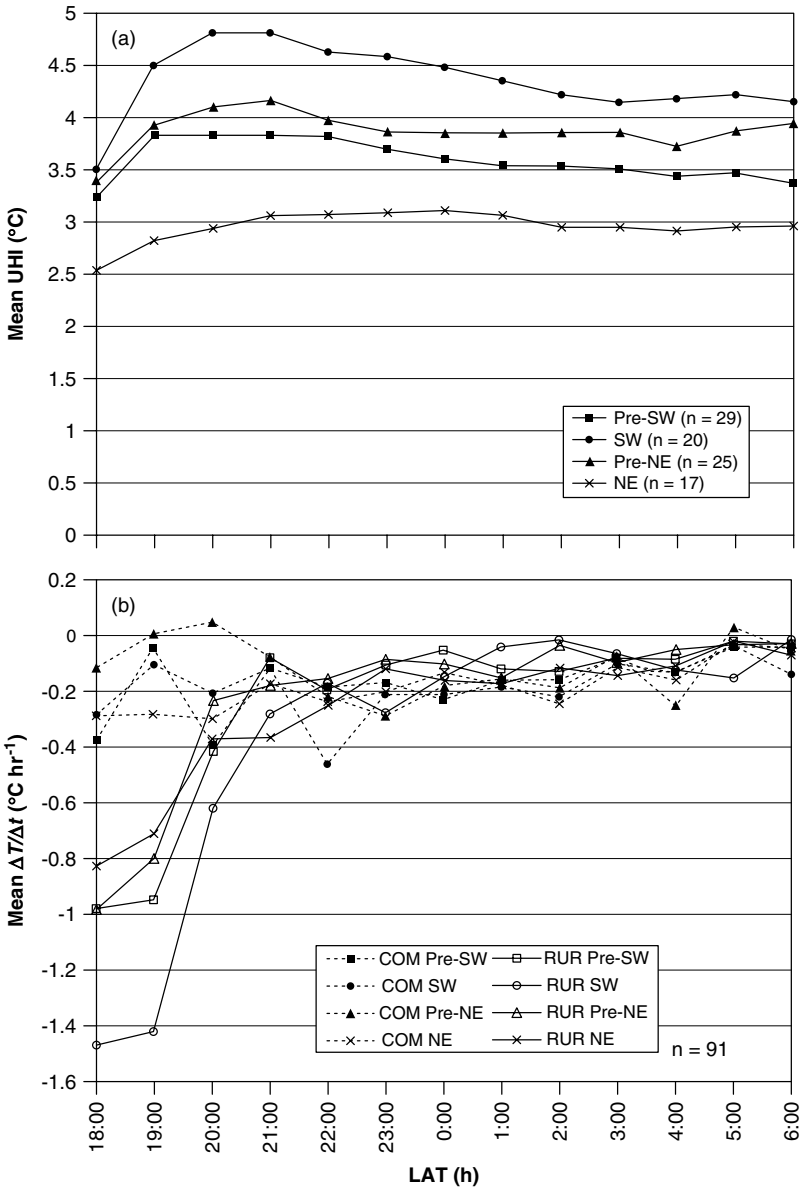

Figure 8. Variation of (a) nocturnal UHI intensity at COM and (b) warming/cooling rates for COM and RUR under clear and calm weather conditions for seasons as defined in Table II. n = number of nights

DOI: 10.1002/joc

cover was <1 okta, and $\overline{u} < 1$ m s^{-1} as documented at MSD Changi Station, and ensemble averages of nocturnal UHI and cooling rates were plotted (Figure 8). Clear seasonal differences are evident in diurnal UHI intensities, with the SW monsoon season having the highest UHI magnitudes, followed by pre-NE, pre-SW, and NE monsoon seasons, respectively (Figure 8(a)). UHI_{MAX} peaks about 3 h after sunset for pre-SW, SW, and pre-NE monsoon seasons and at midnight during the NE monsoon season.

Closer examination of corresponding mean nocturnal $\Delta T/\Delta t$ between COM and RUR also reveals distinct seasonal variations (Figure 8(b)). Magnitudes of mean urban $\Delta T/\Delta t$ remain generally steady at $<0.2\,^{\circ}$C h^{-1} during SW, pre-NE, and pre-SW seasons. However, urban cooling immediately after sunset in the NE monsoon season had twice the magnitude compared to other seasons, before decreasing and matching other seasonal urban cooling rates at ~21 : 00 h. This, combined with relatively low rates of rural cooling in this season, explains the low UHI intensities documented during the NE monsoon. On the other hand, the highest rural $\Delta T/\Delta t$ rates after sunset were observed during the SW monsoon, which, together with relatively low urban cooling rates, explains the higher UHI intensities seen during this season. All rural cooling rates decrease in magnitudes similar to urban cooling rates after 23 : 00 h by which time the fluctuations in UHI intensity were minimal.

3.3. Meteorological impacts on the urban heat island

Various studies have shown the impact of cloud cover and wind speed on UHI intensity (e.g. Ackerman, 1985; Eliasson, 1996; Figuerola and Mazzeo, 1998; Magee *et al.*, 1999). In the present study, UHI intensities were compared with relevant meteorological parameters to determine if similar relationships exist. The only 24-h cloud cover data available was based on observations from MSD Changi Station. However, given the small scale and short lifespan of convective weather systems typical of equatorial climates, data from this station, particularly during daytime, will not be representative for the entire island. Further, on the basis of visual observations, nights were often clear or were associated with high cloud cover. Because of the absence of comprehensive cloud cover data, no systematic analysis of cloud impacts on UHI intensity was therefore attempted.

Similar to the cloud data, observations of wind speed from Changi Airport are not necessarily representative of the island-wide wind field for a given time of day, and wind observations taken at urban sites are greatly influenced by the local-scale urban morphology. Nonetheless, the MSD Changi wind speed observations are assumed to be sufficiently representative for an initial analysis. Mean wind speed was classified into four

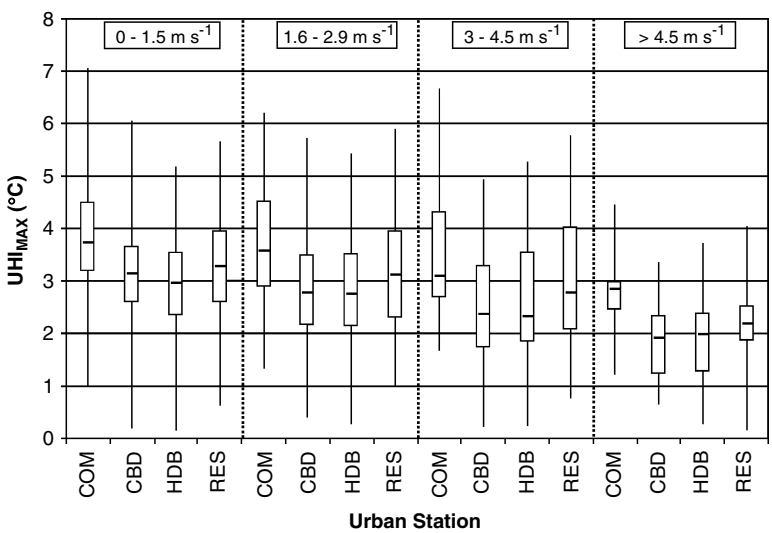

Figure 9. Box plot of nocturnal UHI_{MAX} on cloud-free nights with wind speed data from MSD Changi station. The horizontal bar is median UHI_{MAX}, the box contains 50% of the data including the upper and lower quartiles, and the end points of vertical lines denote extremes

DOI: 10.1002/joc

categories and related to the daily UHI_{MAX} for cloud-free days (Figure 9). Higher maximum UHI intensities at all sites were generally associated with lower wind speeds. This is similar to results from other cities; however, the relationship is not as strong as the one shown by Oke (1998).

4. DISCUSSION

4.1. Urban–rural differences in thermal admittance

UHI arises from differences in the rates of rural *versus* urban cooling (Figure 6), which derives from the differing thermal behaviour of rural and urban surfaces. The thermal behaviour of a surface can be characterised by its thermal admittance (μ). Materials that comprise the urban mosaic generally store or release energy at lower rates compared to soils in rural areas, resulting in a more conservative thermal climate. The higher values of urban thermal admittance (μ_{urban}) compared to rural thermal admittance (μ_{rural}) are reflected in the slower rates of urban temperature changes observed compared to the larger temperature changes in the rural areas, especially at sunset and sunrise.

To estimate mean μ_{rural} of the soil at the rural site, a derivation of the Brunt (1941) equation was used:

$$\Delta T_{t-s} = -\frac{2}{\pi^{1/2}} \left(\frac{L^*}{\mu^{1/2}} \right) t^{1/2} \tag{1}$$

where ΔT_{t-s} is decrease of temperature over time (t) from sunset and L^* is net long-wave radiation flux density. This equation assumes no advection, which should hold given the large size of the rural area. Further, the calculations are done for clear and calm nights only. Night-time L^* data at RUR was obtained from the Q^* observations. Values of mean monthly μ_{rural} ranged from 1000 J m^{-2} s$^{-1/2}$ K^{-1} during drier months (May–July) to 1400 J m^{-2} s$^{-1/2}$ K^{-1} in wetter months (November–January). This is at the lower end of the estimates obtained from a rural area near Vancouver of 1050–2350 J m^{-2} s$^{-1/2}$ K^{-1} (Runnalls and Oke, 2000). Representative values for μ_{urban} are difficult to obtain because of the different materials used in the urban landscape (concrete, tarmac, glass, etc.) (Oke and Maxwell, 1975). They are likely to be larger, as for instance, a dense concrete slab has a value of 2800 J m^{-2} s$^{-1/2}$ K^{-1} (Oke, 1981), and probably change less over time compared to rural values.

Cities as a whole are generally impermeable surfaces, and together with efficient drainage systems will minimise infiltration and surface accumulation of precipitation. In contrast, variations of soil moisture will strongly affect μ_{rural} over time. Surface and soil moisture have previously been cited as key factors in controlling UHI intensity and dynamics (Oke *et al.*, 1991; Imamura, 1993; Runnalls and Oke, 2000), and are able to explain the seasonal variability of UHI magnitudes observed (Figures 7 and 8). Highest UHI intensities occur during drier periods of the year (i.e. the SW monsoon) similar to the results from observations of UHI in other tropical cities (e.g. Padmanabhamurty, 1986; Adebayo, 1987; Jauregui, 1997). Under ideal meteorological conditions, the largest magnitudes of rural cooling rates are also observed during the dry SW monsoon season when μ_{rural} is lowest (Figure 8(b)). This, together with low rates of urban cooling, explains the large and rapid growth of UHI in the early evening. In contrast, low rates of rural $\mathbf{\Delta}T/\mathbf{\Delta}t$ are associated with high μ_{rural} values resulting from frequent and intense precipitation events during the NE monsoon season (Figure 1; Table III). This partly explains the lower magnitudes and slower growth of the UHI during this rainy season.

4.2. Intra-urban differences in UHI intensity

Several factors contribute to differences in intra-urban UHI magnitudes and temporal dynamics. They include variations in surface morphology, local-scale wind speed, green space, and anthropogenic heat emission.

Variations in UHI intensity within urban areas can be related to differences in urban morphology. The geometry of the urban canyon, i.e. the combination of walls, floor, and air volume contained between two

DOI: 10.1002/joc

buildings, is a significant factor in determining UHI intensities (Oke, 1982). A strong relationship between canyon geometry (e.g. H/W, and sky view factor, Ψ_S) and UHI_{MAX} is often observed in temperate cities (Oke, 1981; Eliasson, 1994). Canyons with higher H/W generally absorb and store more incoming short-wave radiation, and emit less long-wave radiation at night. However, no clear relationship can be observed in the present study, as the location with lowest Ψ_S (CBD) is not associated with highest UHI_{MAX}. Further, lowest UHI_{MAX} values are always observed at HDB, which, however, does not have highest Ψ_S (Figure 6; Table I). Moreover, while canyon geometry is a significant factor in increasing absorption of short-wave radiation, very high (low) values of H/W (Ψ_S) will reduce the quantity of energy stored within urban canyons during daytime because of shading (Oke, 1987). Hence the rate of heat storage release at night is less as compared to other areas with lower H/W, possibly explaining the fact that the highest UHI_{MAX} in the present study was not found at CBD. Shading due to tall buildings there may also explain the prominent cool island observed through most of the daytime (Figure 6(a)). In the present study, canyon geometry alone cannot explain the observed intra-urban differences, and other factors must be considered.

To assist the discussion of the intra-urban UHI differences, nocturnal wind speeds taken at each urban site (u) were summarised for each season (Table IV). These observations are not representative of the general land use around each station (i.e. Oke, 2004). However, they provide an estimate of the prevailing wind conditions in the immediate site vicinity. During most seasons, mean site u were highest at HDB, followed by those at RES, CBD, and COM, respectively. This wind speed data, together with other factors such as green space, proximity to water bodies, and anthropogenic heat, will be used in the following discussion.

The relatively high observed u, together with high amounts of green space (Table I), may explain the low UHI intensities found at HDB. Vegetation has been shown to have a mitigating impact on T_u (e.g. Landsberg, 1976; Jauregui, 1990/1991) because the presence of grass, shrubs, and/or trees lowers the collective value of μ_{urban} and also increases the latent heat flux from greater evapotranspiration, resulting in less heat storage within the urban canopy. In Singapore, public residential estates similar to the HDB site generally have designated areas for green spaces (i.e. parks, open grass fields) for various aesthetic, social, and environmental reasons. A 1-ha park is located within 100 m of the HDB site, with trees of 5 m height and shrubs planted in a regular and managed fashion throughout the area. Given the relative high u recorded, it is possible that the immediate area around the HDB site experiences advection of cooler air from the surrounding green spaces, lowering UHI intensity.

As discussed above, the CBD site is subject to substantial shading. In addition, the proximity to local water bodies, i.e. the Singapore River (~200 m N) and coast (~500 m E and ~1 km S), exposes this site to advection of cooler air throughout the year which may account for relatively lower UHI intensities observed here. This effect is largest during the SW monsoon, which is characterised by southerly winds (Figure 5) with a predominant fetch over the Singapore Straits, resulting in lowest mean UHI_{MAX} intensities of all sites documented during this period (Figure 7). Similar advective cooling has been observed in Kuwait City, Kuwait (Nasrallah *et al*., 1990), and in Vancouver (Runnalls and Oke, 2000).

In contrast, absence of local-scale ventilation at RES could account for the relatively higher UHI intensities recorded despite the low site H/W. A cluster of high-rise residential flats of $z = 80–120$ m is located 1 km S of the site, possibly blocking the nocturnal wind circulation between RES and the southern coast 1.5 km away. During the SW monsoon, the mean u at RES are lower as compared to HDB, which is located at the same distance from the coast but does not have a similar potential blocking effect due to buildings.

Table IV. Mean nocturnal local wind speed recorded at urban stations between March 2003 and March 2004

Station	Pre SW monsoon ($m\ s^{-1}$)	SW monsoon ($m\ s^{-1}$)	Pre NE monsoon ($m\ s^{-1}$)	NE monsoon ($m\ s^{-1}$)	All seasons ($m\ s^{-1}$)
COM	0.56	0.70	0.61	0.52	0.60
CBD	0.57	0.80	0.73	0.87	0.74
HDB	N.A.	1.17	0.85	0.74	0.92
RES	N.A.	0.86	0.66	1.09	0.87

DOI: 10.1002/joc

This wind-break effect, however, is absent during the NE monsoon when RES experiences higher mean u compared to HDB.

UHI intensities are consistently highest at COM despite the lower H/W compared to CBD. Generally, lower wind speeds and absence of advective cooling may in part explain this result. It is also possible that variations in anthropogenic heat (Q_F) contribute to the observed differences. Sailor and Lu (2004) attribute anthropogenic heat emissions to three main sources:

$$Q_F = Q_V + Q_B + Q_M \tag{2}$$

where Q_V = excess heat from vehicles, Q_B = waste heat due to electrical consumption and/or point-of-use heating from buildings or air cooling systems, and Q_M = heat from human metabolism. The COM site is located in an area of very high commercial activity (Table I), which usually continues until 22 : 00 h. In contrast, the CBD, which primarily houses offices, is relatively devoid of commercial activity after 19 : 00 h. All three sources on the right-hand side of Equation (2) are likely to be higher at COM compared to CBD from about 19 : 00–22 : 00 h, which could explain the relatively early peak and larger magnitude of the UHI at COM compared to other urban sites (Figure 6(a)). The level of activity starts to decrease at around 22 : 00 h when most commercial businesses (i.e. shopping malls) cease operations. This corresponds to the notable decrease of $\Delta T/\Delta t$ observed at this time (Figure 6(b)). Anthropogenic activity has also been used to explain the early evening peak in the UHI in Mexico City (Jauregui, 1997) and the pre-sunrise UHI maxima in the Indian cities of Delhi (Padmanabhamurty and Bahl, 1982) and Pune (Padmanabhamurty, 1979). The last two studies suggest that the variations in anthropogenic heat are mainly due to increases in traffic during the early morning.

4.3. Comparison of the results with other studies

Similar to findings from past studies on Singapore UHI (Nieuwolt, 1966; SMS, 1986; Goh and Chang, 1998; Wong and Yu, 2005), the largest nocturnal ΔT_{u-r} was consistently found in the commercial area of Orchard Road. The seasonal variation of UHI intensity is also comparable to previous observations by SMS (1986) and Goh and Chang (1998), with highest intensities observed during the SW monsoon season. UHI_{MAX} occurs 3–4 h after sunset at COM, and occurs approximately during the time used by most previous Singapore studies for observations. Other urban stations, on the other hand, have UHI_{MAX} occurring around midnight. The results from the present study are true for both ideal and all-weather conditions. Past and present results mostly observed at 21 : 00 h for different seasons are summarised in Table V. In order to compare with present results, the previous studies have their findings converted from LT to LAT. Also included are the present UHI_{MAX} values for each season irrespective of the time of occurrence. The present results are 2–3 °C higher than the observations from earlier studies. Some of this difference may be attributed to less than ideal meteorological conditions, which were often not explicitly stated.

UHI_{MAX} obtained under ideal conditions plotted against the logarithm of city population tend to follow a linear relationship (Oke, 1973). Regression coefficients are different for different city morphologies

Table V. Comparison of UHI_{MAX} values for each season in Singapore from past and present studies

Study/time of UHI_{MAX} (LAT)	Pre-Southwest monsoon (°C)	Southwest monsoon (°C)	Pre-Northeast monsoon (°C)	Northeast monsoon (°C)
Nieuwolt (1966)/~22 : 00	N.A.	N.A.	~4.5	N.A.
SMS (1986)/~21 : 00	N.A.	~5	N.A.	<2.5
Goh and Chang (1998)/~21 : 00	3.5	4.8	3.3	2.5
Wong and Yu (2005)/~01 : 00–03 : 00	N.A.	N.A.	~4	N.A.
Present study/21 : 00 only	5.84	7.07	6.07	5.49
Present study/any hour	6.84	7.07	6.58	5.91

DOI: 10.1002/joc

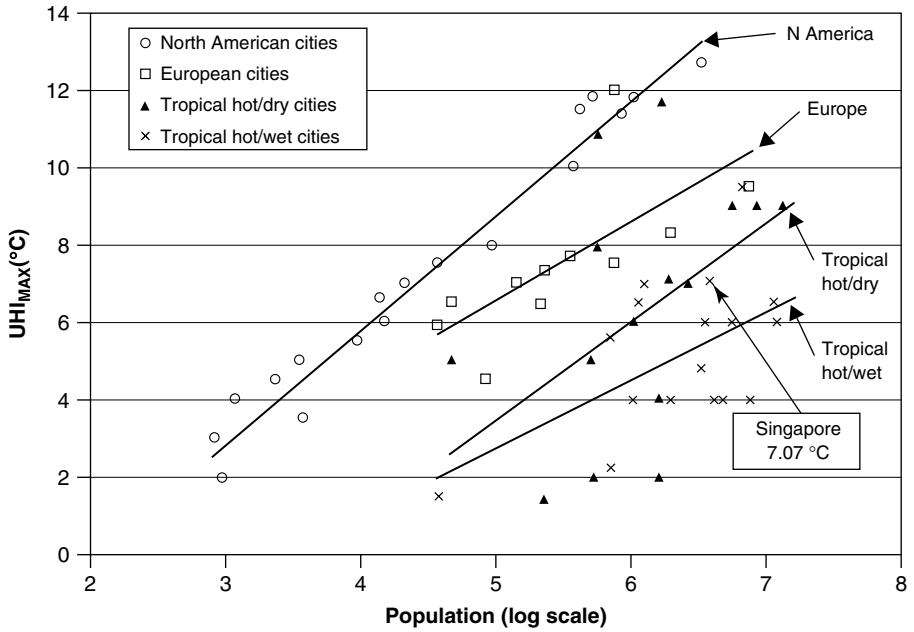

Figure 10. UHI_{MAX} plotted against city population. Different symbols are used for cities in different climate zones. Solid lines are the corresponding regression lines (After Oke, 1973 and Jauregui, 1986a). Tropical hot/wet cities include those with Köppen classification *Af, Am*, and tropical hot/dry cities include those with *Aw, BSh, BWh, Cwa,* and *H*

(e.g. North American and European cities) and climates (e.g. temperate *vs* tropical hot/dry *vs* tropical hot/humid). The present UHI_{MAX} value lies at the upper end of the range of values for tropical hot/wet cities, but is lower than that of cities with a similar population located in tropical hot/dry and temperate climates (Figure 10). Variations in UHI_{MAX} between temperate and tropical cities have been previously explained by higher surface albedo (e.g. lighter coloured rooftops) and lower thermal emissivity (e.g. from corrugated rooftop iron sheets) of tropical urban building materials (Oke, 1986), which could be the case for cities in less developed tropical countries. However, this may not apply to cities in developed tropical countries, e.g. Singapore and Hong Kong, which use building materials similar to those of European or North American cities. Further reasons may include lower levels of tropical anthropogenic combustion and higher air pollution in tropical cities (Oke *et al*., 1991). Again, this may not necessarily apply to Singapore.

The key factor for the observed differences in UHI_{MAX} among cities in different climate regions is probably variations in moisture conditions of the respective rural surroundings (Oke, 1986; Oke *et al*., 1991; Imamura, 1993). Tropical hot/wet cities experience greater amounts of annual precipitation than mid-latitude cities, which is associated with a corresponding increase in soil moisture and high μ_{rural} values which result in lower UHI_{MAX}. Similarly, tropical hot/dry cities generally have higher magnitudes of UHI_{MAX} than tropical hot/wet cities primarily because of the lower levels of soil moisture during the dry season, which initiates more rapid cooling of the rural surface after sunset.

5. SUMMARY AND CONCLUSION

The temporal dynamics of the UHI in Singapore has been analysed using hourly data from four urban and one rural station recorded over a period of 1 year. The main findings from this study are:

(1) Maximum UHI intensities are found in the COM (Orchard Road) at approximately 21 : 00 LAT (22 : 00 LT), with the highest UHI intensity of 7.07 °C measured on 17 May 2003. At other sites (CBD, high-rise residential estate, and low-rise residential area) mean UHI intensities were lower and reached a maximum

DOI: 10.1002/joc

approximately 6 h after sunset. These results were observed under both 'ideal' conditions of clear and calm weather as well as for all weather conditions.

(2) There is distinct seasonal variability in the data for all sites. Generally, higher UHI intensities were observed during the relatively drier months associated with the southwest monsoon season (May–August) and lowest intensities during the wet northeast monsoon season (December–January). Intermediate UHI intensities were measured during the inter-monsoon periods.

(3) The seasonal variability in the UHI intensity can be explained by the variability of moisture content of the undeveloped, rural reference site, which is largely influenced by the seasonal variation of precipitation. The observations show higher (lower) rural thermal admittance during the wet NE monsoon season, which results in lower (higher) rural cooling rates and hence lower (higher) UHI intensities.

(4) The relationship between urban canyon geometry and UHI intensity is weaker than expected. A combination of other site-specific factors such as anthropogenic heat, amount of green space, and distance to water bodies is suggested to explain why UHI intensity is highest, and occurs earlier in the commercial district rather than in the CBD.

(5) The inverse relationship seen between surface wind speed and UHI intensity under cloudless conditions is small. The site-specific factors mentioned in (4) seem to be more important in explaining the differences in intra-urban UHI intensities than meteorological conditions.

This study is one of the first and most comprehensive investigations of the canopy-level UHI of an equatorial city. Its findings will be a useful addition to the formation of a body of tropical urban climate knowledge as first proposed by Oke *et al*. (1990/1991).

ACKNOWLEDGEMENTS

The authors would like to thank the Land Transport Authority, Bedok Town Council, and the Ministry of Defence of Singapore for their permission to install sensors on their property. Mr J. Tan from the Meteorological Services Division, National Environmental Agency assisted in provision of secondary data. Mrs L. K. Lee (National University of Singapore) helped with Figure 3. Helpful comments from reviewers are also acknowledged. Funding for this study was provided by the National University of Singapore (R-109-000-037-112).

REFERENCES

Ackerman B. 1985. Temporal march of the Chicago heat island. *Journal of Climate and Applied Meteorology* **24**: 547–554.

Adebayo YR. 1987. Land-use approach to the spatial analysis of the urban "heat island" in Ibadan, Nigeria. *Weather* **42**: 273–280.

Brunt D. 1941. *Physical and Dynamical Meteorology*. Cambridge University Press: London.

Chandler TJ. 1965. *The Climate of London*. Hutchinson: London.

Chia LS, Foong SF. 1991. Climate and weather. In *The Biophysical Environment of Singapore*. Chia LS, Rahman A, Tay DBH (eds). Singapore University Press and the Geography Teachers' Association of Singapore: Singapore; 13–49.

Deosthali V. 2000. Impact of rapid urban growth on heat and moisture islands in Pune city, India. *Atmospheric Environment* **34**(17): 2745–2754, DOI: 10.1016/S1352-2310(99)00370-20.

Department of Statistics. 1998. *Yearbook of Statistics, Singapore*. Department of Statistics: Singapore.

Eliasson I. 1994. Urban-suburban-rural air temperature differences related to street geometry. *Physical Geography* **15**(1): 1–22.

Eliasson I. 1996. Intra-urban nocturnal temperature differences: a multi-variate approach. *Climate Research* **7**: 21–30.

Figuerola PI, Mazzeo NA. 1998. Urban-rural temperature differences in Buenos Aires. *International Journal of Climatology* **18**(15): 1709–1723, DOI: 10.1002/(SICI)1097-0088(199812)18 : 15<1709::AID-JOC338>3.0.CO;2-I.

Goh KC, Chang CH. 1998. The nocturnal heat island phenomenon of Singapore revisited. In *Paper Presented at the 5th Southeast Asian Association Geographers' Conference*, Singapore.

Goldreich Y. 1984. Urban topoclimatology. *Progress in Physical Geography* **8**(3): 336–364.

Imamura IR. 1993. Role of soil moisture in the determination of urban heat island intensity in different climate regimes. In *Air Pollution*. Zannetti P, Brebbia CA, Garcia Gardea JE, Ayala Milian G (eds). Computational Mechanics and Elsevier Science: Southampton, Boston, London and New York.

Jauregui E. 1973. The urban climate of Mexico City. *Erdkunde* **27**: 298–306.

Jauregui E. 1986a. Tropical urban climates: review and assessment. *Urban Climatology and its Applications with Special Regard to Tropical Areas*, *World Climate Programme, WMO Publication No. 652*. World Meteorological Organisation: Geneva; 26–45.

Jauregui E. 1986b. The urban climate of Mexico City. *Urban Climatology and its Applications with Special Regard to Tropical Areas*, *World Climate Programme, WMO Publication No. 652*. World Meteorological Organisation: Geneva; 63–86.

Jauregui E. 1990/1991. Influence of a large urban park on temperature and convective precipitation in a tropical city. *Energy and Buildings* **15**(3–4): 457–463, DOI: 10.1016/0378-7788(90)90021-A.
Jauregui E. 1997. Heat island development in Mexico City. *Atmospheric Environment* **31**(22): 3821–3831, DOI: 10.1016/S1352-2310(97)00136–2.
Jauregui E, Godinez L, Cruz F. 1992. Aspects of heat-island development in Guadalajara, Mexico. *Atmospheric Environment* **26B**(3): 391–396.
Landsberg HE. 1976. *Weather, Climate, and Human Settlements*, *WMO Special Environmental Report No. 7*. World Meteorological Organisation: Geneva.
Landsberg HE. 1981. *The Urban Climate*. Academic Press: New York.
Lowry WP. 1977. Empirical estimation of urban effects on urban climate: a problem analysis. *Journal of Applied Meteorology* **16**: 129–135.
Ludwig FL. 1970. Urban temperature fields. *WMO Technical Note 108: Urban Climates*. World Meteorological Organisation: Geneva; 80–108.
Magee N, Curtis J, Wendler G. 1999. The urban heat island effect at Fairbanks, Alaska. *Theoretical and Applied Climatology* **64**(1–2): 39–47, DOI: 10.1007/s007040050109.
Nakamura Y, Oke TR. 1988. Wind, temperature and stability conditions in an east-west orientated urban canyon. *Atmospheric Environment* **22**: 2691–2700.
Nasrallah HA, Brazel AJ, Balling RC Jr. 1990. Analysis of the Kuwait City urban heat island. *International Journal of Climatology* **10**: 401–405.
Nieuwolt S. 1966. The urban microclimate of Singapore. *Journal of Tropical Geography* **22**: 30–37.
Oke TR. 1973. City size and the urban heat island. *Atmospheric Environment* **7**: 769–779.
Oke TR. 1981. Canyon geometry and the nocturnal urban heat island: comparison of scale model and field observations. *Journal of Climatology* **1**: 237–254.
Oke TR. 1982. The energetic basis of the urban heat island. *Quarterly Journal of the Royal Meteorological Society* **108**: 1–24.
Oke TR. 1986. Urban climatology and the tropical city. *Urban Climatology and its Applications with Special Regard to Tropical Areas*, *World Climate Programme, WMO Publication No. 652*. World Meteorological Organisation: Geneva; 1–25.
Oke TR. 1987. *Boundary Layer Climates*, 2nd edn. Methuen: London.
Oke TR. 1998. An algorithmic scheme to estimate hourly heat island magnitude. *Proceedings from the 2nd Urban Environment Symposium*. American Meteorological Society: Albuquerque, NM, Boston, MA; 80–83.
Oke TR. 2004. Initial guidance to obtain representative meteorological observations at urban sites. IOM Report No.81, WMO/TD. No. 1250. World Meteorological Organization: Geneva.
Oke TR, Maxwell GB. 1975. Urban heat island dynamics in Montreal and Vancouver. *Atmospheric Environment* **9**: 191–200.
Oke TR, Taesler R, Olsson LE. 1990/1991. The tropical urban climate experiment (TRUCE). *Energy and Buildings* **15–16**: 67–73, DOI: 10.1016/0378-7788(90)90117-2.
Oke TR, Johnson GT, Steyn DG, Watson ID. 1991. Simulation of surface urban heat islands under "ideal" conditions at night, part 2: diagnosis of causation. *Boundary-Layer Meteorology* **56**: 339–358.
Padmanabhamurty B. 1979. Isotherms and isohumes in Pune on clear winter nights: a mesometeorological study. *Mausam* **80**(1): 134–138.
Padmanabhamurty B. 1986. Some aspects of the urban climates of India. *Urban Climatology and its Applications with Special Regard to Tropical Areas*, *World Climate Programme, WMO Publication No. 652*. World Meteorological Organisation: Geneva; 136–165.
Padmanabhamurty B, Bahl HD. 1982. Some physical features of heat and humidity islands at Delhi. *Mausam* **33**(2): 211–216.
Runnalls KE, Oke TR. 2000. Dynamics and controls of the near-surface heat island of Vancouver, British Columbia. *Physical Geography* **21**(4): 283–304.
Sailor DJ, Lu L. 2004. A top-down methodology for developing diurnal and seasonal anthropogenic heating profiles for urban areas. *Atmospheric Environment* **38**(17): 2737–2748, DOI:10.1016/j.atmosenv.2004.01.034.
Sham S. 1987. The urban heat-island – its concept and application to Kuala Lumpur. In *Urbanization and the Atmospheric Environment in the Low Tropics: Experiences from the Kelang Valley region, Malaysia*, Sham S (ed). Pernerbit Universiti Kebangsaan Malaysia: Kuala Lumpur; 242–253.
Singapore Meteorological Service. 1986. A study of the urban climate of Singapore. In *The Biophysical Environment of Singapore and its Neighbouring Countries*, Chia LS, Lee HC, Rahman AR, Tong PL, Woo WK (eds). Geography Teacher's Association: Singapore; 50–76.
Singapore Meteorological Service. 1967–1988. *Summary of Observations*, Various issues. Meteorological Services: Singapore.
Taesler R. 1980. *Studies of the Development and Thermal Structure of the Urban Boundary Layer in Uppsala. Part II, Data Analysis and Results*, No. 61. Swedish Meteorological Institute: Uppsala.
Wong NH, Yu C. 2005. Study of green areas and urban heat island in a tropical city. *Habitat International* **29**: 547–558, DOI: 10.1016/j.habitatint.2004.04.008.
World Meteorological Organization. 1971. *Guide to Meteorological Instrument and Observing Practices*, 4th edn. World Meteorological Organization: Geneva.